Broadband spike excitation method for in-liquid QCM sensors

Pablo Resa, Pedro Castro, Jaime Rodríguez-López and Luis Elvira

Centro de Acústica Aplicada y Evaluación No Destructiva (CAEND), UPM-CSIC

C/Serrano 144, 28 006 Madrid, Spain

Phone number: (+34) 915618806(104)

Fax number: (+34) 914117651

Email: pablo.resa@caend.upm-csic.es, luis.elvira@caend.upm-csic.es

Abstract

A Quartz Crystal Microbalance (QCM) is a highly sensitive device based on the measurement of the resonance parameters of a thickness-shear piezoelectric resonator, which classical application is the detection of attached mass per unit area. Although the most economical ways of driving these sensors make use of oscillator circuits, other electronic interfaces are also well-established, i.e., electrical impedance analysis and impulse excitation/decay methods. Impulse excitation and decay methods are founded on the same principle, but in practice only the latter has been exploited. The present work explores the suitability of a broadband spike excitation technique (up to 0.25 GHz) as an interface electronic system for QCM sensors. The principles of measurement —including the processing of signals— are described in detail and illustrated for liquids with different mechanical shear impedances. The proposed mode of operation has proved some advantageous characteristics: both resonant frequency and energy dissipation can be simultaneously determined in a wide range of frequencies; it is appropriate for in-liquid sensing applications (including highly viscous liquids); it can be easily automated for continuous monitoring and integrated with other external circuitry (such as multiplexing for sensor arrays).

Keywords: Quartz Crystal Microbalance; AT-cut quartz crystal; Thickness-Shear Mode resonator; Shear impedance spectroscopy; Impulse excitation method; Ultrasonic characterization

1 Introduction

Quartz Crystal Microbalances (QCM), sometimes referred to as Thickness-Shear Mode (TSM) sensors, are probably the most widespread and versatile ultrasound-based analytical technique. Typical applications include the measurement of deposition rate and film thickness, the investigation of surface reactions and the study of viscoelastic properties [1]. A very important aspect of these resonators is the interface circuitry, commonly divided into three broad categories: oscillators, network analyzers and impulse/decay methods [1-4]. In spite of some drawbacks, mostly related to the interference of the electronic components, oscillator circuits are habitually preferred in most cases because of their low price, integration capability, high resolution and fast response. Impedance network analyzers provide more complete information, but they are normally restricted to laboratory environments owing to their high cost and large dimensions. Impulse excitation and decay methods are based on the same principle and their main feature is that the resonance parameters are not much influenced by the electronic network, since the crystal is freely oscillating during the measurement. In practice, only the latter (decay method) is used, being at the root of the QCM with dissipation monitoring technique [5-7]. With the increasing QCM applications in liquid media, new advances in these excitation systems have been proposed (for instance, [8-12]). However, apart from some brief references, the impulse excitation method, has not yet been studied or reported in depth. Some limitations occasionally attributed to this interface are: (1) high expenses for circuitry, (2) ideal pulse front slopes are difficult to achieve, (3) other harmonics different from that desired are excited and additional circuitry is necessary, (4) limited range for precise frequency and damping measurement, (5) not appropriate for in-liquid applications, and (6) complex signal

processing involved. The present work analyzes in detail the performance, limitations and measurement principles of a broadband spike (impulse) excitation method to interrogate thickness-shear piezoelectric crystals with application to liquid media. Experimental results of the resonant frequencies and bandwidths for diverse pure liquids (up to 0.25 GHz) are presented.

2 Materials and methods

2.1 Experimental setup

The experimental setup is depicted in Fig. 1 and consisted of the following elements:

- QCM cell made up of an AT-cut quartz crystal provided by CH Instruments Inc., USA (7.995 MHz fundamental frequency, 13.7 mm blank diameter, 5.1 mm electrode diameter, polished surface finish, 100 Å Ti & 1 000 Å Au electrode material, keyhole electrode pattern).

- 200 MHz (-3 dB) Panametrics ultrasonic pulser/receiver, model 5900PR (P/R mode, 2 kHz PRF, 1 μJ energy, 50 Ω damping, 1 MHz HP filer, 200 MHz LP filter, 0 dB attenuators, 26 dB gain, 0º RF output phase).

- 500 MHz, 500 MSa/s and 8 bits Tektronix TDS520 digitizing oscilloscope (15 000 points record length, 50 ns/div delayed scale, 1 024 signals average rating).

- Personal computer connected to the oscilloscope via an Agilent 82357A USB/GPIB interface.

The measuring principle is similar to the previously described for thickness-expansion mode (TEM) resonators [13]. The experimental cell was made up of a 1 mL screw top tube with the quartz disk silicone glued to the bottom (Fig. 2). The electrodes of the piezoelectric transducer were soldered to an RF coaxial cable using copper strips (the side in contact with the liquid was grounded). The active surface area of the quartz was left intact to ensure that the mounting elements did not significantly alter the

resonant parameters. The measuring cell was waterproofed and immersed into a Julabo FP45HE refrigerated/heating circulator bath set at 25.00±0.01 ºC. The programming environment LabVIEW has been used to record the output signals and process the collected data for visualization.

2.2 Electrical equivalent circuit

The ultrasonic pulser/receiver generates a voltage spike, by means of a capacitive discharge, driving the QCM sensor. Although the pulser is a complex electrical network that also amplifies and filters the electrical response, it can be converted into a Thévenin equivalent circuit —assuming linearity— comprising only one voltage source, V_P, and one impedance, Z_P. A circuit representation of a spike pulser and its characteristics can be found in [14]. In the vicinity of resonances, the behavior of an air-backed QCM sensor loaded with a liquid, $Z_L = R_L + j\omega L_L$, can be described by the extended Butterworth-van Dyke equivalent circuit, containing two parallel branches (Fig. 3). The left-hand branch corresponds to the static dielectric capacitance, $C_{Q,0}$, and the right-hand one is related to the mechanical response of the piezocrystal. The expressions relating the electrical components of Fig. 3 to the mechanical properties of a loaded TSM resonator can be found elsewhere (for instance, [1, 4]).

The output voltage, V, is given by:

$$V = V_P \frac{Z_{eq}}{Z_P + Z_{eq}}, \tag{1}$$

where

$$Z_{eq} = \left(j\omega C_{Q,0} + \frac{1}{j\omega L_Q + \frac{1}{j\omega C_Q} + R_Q + Z_L} \right)^{-1} \quad (2)$$

Since the impedance of the ultrasonic pulser is around 30 Ω [14], and considering that near the resonances $Z_{eq} >> Z_P$ [4], it follows that:

$$V = V_P \frac{1}{1 + Z_P / Z_{eq}} \approx V_P \left(1 - Z_P Y_{eq}\right), \quad (3)$$

where $Y_{eq} = \frac{1}{Z_{eq}}$ is the equivalent admittance of the loaded resonator. The maxima of the voltage peaks correspond to the maximal admittance values.

In an ideal series RLC circuit, the quality factor is:

$$Q = \frac{1}{R}\sqrt{\frac{L}{C}}. \quad (4)$$

For typical values of an AT-cut quartz crystal (R_Q=10 Ω, $C_{Q,0}$=7 pF, L_Q=6 mH, C_Q=45 fF), the Q factor can be approximated by the expression:

$$Q \approx \frac{1}{\left(R_P + R_Q + R_L\right)}\sqrt{\frac{L_Q + L_L}{C_Q}}, \quad (5)$$

and the bandwidth, $B_w = \frac{f_0}{Q}$, results in:

$$B_w \approx f_0 \left(R_Q + R_P + R_L\right)\sqrt{\frac{C_Q}{L_Q + L_L}}. \quad (6)$$

Given that $L_Q >> L_L$ [1], then:

$$\Delta B_w \propto \Delta R_L \,. \tag{7}$$

Additionally, there are some considerations to be taken into account:

– To a first approximation, the spectrum generated by the pulser/receiver can be assumed constant over narrow bandwidths (i.e., a Dirac delta function in the time domain), which might not hold for heavily damped resonators. An explicit and more accurate Fourier transform of V_P can be found in [14].

– In a typical spike pulser, the energy is stored in a capacitor and discharged at the repetition rate by closing a switch. In this sense, this interface differs from the traditional decay method, where the signal excitation is intermittently disconnected by opening a relay.

– The configuration of a pulser has to be preserved over all the measurements, since the equivalent impedance of these electronic devices changes significantly in both amplitude and shape with the settings.

– The imaginary part of the pulser impedance, coming from the storage capacitor, can slightly perturb the absolute value of the resonant frequency (although without significantly affecting the changes in frequency or bandwidth).

2.3 Signal processing

Fig. 4 depicts the waveform of the electrical signals displayed on the oscilloscope and its frequency spectrum. All the harmonics within the bandwidth of the electronic excitation can be clearly perceived. In a close view, the output signals significantly

differ from an ideal exponentially decaying sinusoidal function at all the frequency components due to the interference of spurious modes. These wave patterns, resulting from the superposition of different waves, make the extraction of the resonant parameters difficult. Hence, the signal processing chosen is detailed next (implemented in MATLAB):

2.3.1 Resonant frequencies

To determine the resonant frequencies, a temporal interval (1-30 μs) has been selected after analyzing the stability of the instantaneous frequency, calculated as the derivative of the phase of the complex time signal (analytic signal). The signals were multiplied by a 'Hanning window' that was zero-valued outside of the chosen interval. The resonant frequencies have been calculated from the maximum values of the zero-padded Fast Fourier Transform (FFT). The accurate determination of these quantities was performed by using the second-order Goertzel algorithm, which computes more efficiently the discrete Fourier transform (DFT) for a subset of indices.

2.3.2 Bandwidths

The bandwidths, B_w, of each harmonic have been determined from the decay rates. Supposing a monochromatic sinusoidal signal, $u(t)$, of maximum amplitude, u_0, with an exponentially decaying envelope,

$$u(t) = u_0 e^{-\frac{t}{\tau}} \sin\left(2\pi f_0 t + \phi\right), \tag{8}$$

the dissipation factor, D, and the half bandwidth, Γ, are inversely proportional to the decay time constant, τ:

$$D = \frac{1}{Q} = \frac{1}{\pi f_0 \tau}, \quad (9)$$

$$\Gamma = \frac{B_w}{2} = \frac{1}{2\pi\tau}. \quad (10)$$

After removing the DC offset, the output signals of each harmonic were separated applying a digital FFT bandpass filter centered at the corresponding resonant frequency and with a bandwidth of ~3-12 MHz depending on the overtone number. Then, the spectral data were converted back into the time domain via the inverse FFT. The envelopes of each 'monochromatic' signal were obtained from the amplitude of the resulting complex time signal. Since these envelopes were not subject to a pure exponential decay, only the beginnings of the curves were fitted to an exponential function (~1-60 μs).

An important characteristic of the signal treatment described herein is that only a temporal interval has to be analyzed to determine both the resonant frequency and the quality factor. Working with a portion of the signals significantly diminishes the processing time and computing requirements.

2.4 Impedance network analysis

In addition, the resonant parameters of the QCM sensor, loaded with different liquids, have been measured using an Agilent 4294A Precision Impedance Analyzer, ranging from 40 Hz to 110 MHz. The resonant frequencies have been determined from the maxima of the conductance peaks, which correspond to the electrical series resonant frequencies (MSRF) of the equivalent Butterworth Van-Dyke circuit. The bandwidths

have been calculated as the difference between the two frequencies at which the amplitude was half of its maximum value.

2.5 Liquid samples

The following pure liquids have been measured: acetonitrile (Panreac Química, purity >99.9%), *Baysilone*® fluid M 10 (Momentive Specialty Chemicals, 100% polydimethylsiloxane), 1-butanol (Panreac Química, purity >98.5%), ethanol (Quimivita, purity >99.5%), glycerol (Panreac Química, purity >99.5%), lactic acid (Panreac Química, purity >95.0%), methanol (J.T.Baker, purity >99.8%) and 2-propanol (Panreac Química, purity >99.5%). Tap water was purified with an ELGA Purelab UHQ distiller system (>18 MΩ·cm) and degassed in a vacuum chamber. The viscosities and densities of these liquids at 25 ºC have been collected from the literature [15] and are given in Table 1. Liquid samples were selected according to diverse criteria. Since liquid mixtures can lead to additional relaxation phenomena at high-frequencies, only pure liquids with well-known properties were studied. Liquids with different viscosities (such as glycerol, lactic acid, baysilone and acetonitrile) were appropriate to test the validity range of the method, while liquids with low viscosities (such as methanol, water, ethanol and isopropanol) were useful to observe the response to small changes.

3 Results and discussion

The changes in the complex resonant frequency, $\Delta f^* = \Delta f_0 + j\Delta\Gamma$, of a TSM resonator when one face is in contact with a semi-infinite Newtonian liquid, with density ρ_L and viscosity η_L, are given by [16-18]:

$$\frac{\Delta f^*}{f_0} = (-1+j)\sqrt{\frac{Nf_0}{\pi\rho_Q\mu_Q}\eta_L\rho_L}\,, \tag{11}$$

where $\Gamma = \frac{B_w}{2}$ is half bandwidth, f_0 is the fundamental resonant frequency, ρ_Q and μ_Q are the density and rigidity modulus of the quartz crystal (respectively), and $N = 1, 3, 5, 7...$ is the overtone number.

The fundamental resonant frequency (first harmonic), determined using the current spike excitation method, as a function of the square-root of the product of density and viscosity is plotted in Fig. 5 for different liquids with viscosities ranging from 0.3 to 1000 mPa·s. A clear linear dependence can be observed in agreement with previous Eq. (11). Deviations from this equation are comparable to other works (for instance, [17]) and are commonly attributed to the finite size of the piezoelectric element, the contribution of interfacial effects and the electrical/viscoelastic properties of the liquid. Significant changes in the viscosity of a liquid can also be caused by small fluctuations in temperature or impurities. In order to distinguish between the frequency shifts purely due to the liquid loading and other secondary effects, the resonant parameters resulting from the impulse excitation method have been compared to those obtained with an impedance network analyzer. In Fig. 6, it can be seen that both modes of operation give very similar results for the fundamental frequency and higher

harmonics (the slopes are 0.98 and 1.01 for the first and third harmonic, respectively). In this graph, the liquid glycerol has not been included because the electrical conductance peak was flattened and noisy, and its maximum could not be estimated with confidence.

The factor $(-1+j)$ in Eq. (11) implies that the contributions of a pure viscous fluid to frequency and half bandwidth shifts are the same with opposite sign. These two parameters have been determined with the spike method and the results for the fundamental frequency are plotted in Fig. 7. Although these two quantities are not identical, a good correlation between them can be appreciated. In general, the measurement of the resonant frequency gave better results than the decay time constant, especially for highly viscous liquids, on account of the signal-to-noise ratio, computational efficiency and the interference of unwanted modes. For higher harmonics, the relationship between resonant frequency and bandwidth significantly deviates from linearity for several fluids (namely, 1-butanol, *Baysilone*® fluid M 10, lactic acid and glycerol), owing to their non-Newtonian behavior with increasing frequency [19].

Due to the small penetration depth, $\delta = \sqrt{\frac{\eta_L}{\pi \rho_L f}}$, of shear waves in liquids —for instance, the penetration depth in water at 250 MHz is less than 40 nm— measurements at high frequencies using techniques based on the propagation of travelling shear waves (such as through-transmission or pulse-echo) can be very difficult to achieve. The proposed method overcomes this limitation, allowing the simultaneous determination of resonance parameters in a wide range of frequencies and fluids. Fig. 8 shows the

changes in the resonant frequency (pure water as reference) of a QCM sensor loaded with several fluids at 25 ºC. The frequency shifts have been 'normalized' by dividing each value by the square root of the harmonic number (1, 3, 5, 7…). It can be noticed that low viscous liquids do not exhibit dispersion below 250 MHz. As the viscosity increases, the relaxation time increases and the shift in the 'normalized' resonant frequency decreases with frequency (this was the case for the above mentioned liquids). At enough high frequencies, the behavior of liquids is not Newtonian anymore.

Generalizing to viscoelastic media, Eq. (11) becomes:

$$\frac{\Delta f^*}{f_0} = \frac{j}{\pi Z_Q} Z_L^* = \frac{1}{\pi Z_Q}\left(-X_L + jR_L\right), \tag{12}$$

where Z_Q and $Z_L^* = R_L + jX_L$ are the complex mechanical shear impedance of the quartz crystal and the fluid, respectively:

$$\begin{aligned} Z_Q &= \sqrt{\rho_Q \mu_Q} \\ Z_L^* &= \sqrt{\rho_L G_L^*} = \sqrt{j\rho_L \omega \eta_L^*} \end{aligned}. \tag{13}$$

The real and imaginary parts of the shear modulus, $G_L^* = G_L' + jG_L''$, and the viscosity, $\eta_L^* = \eta_L' - j\eta_L''$, are related as follows:

$$\eta_L^* = -j\frac{G_L^*}{\omega} = \frac{1}{\omega}\left(G_L'' + jG_L'\right). \tag{14}$$

Hence, both the dynamic shear viscosity, η_L', and the out-of-phase viscosity (elasticity), η_L'', can be estimated from the measurements of the resonant frequency and half bandwidth shifts:

$$\begin{aligned} \eta_L' &= 2\frac{R_L X_L}{\rho_L \omega} \\ \eta_L'' &= \frac{R_L^2 - X_L^2}{\rho_L \omega} \end{aligned} \quad . \tag{15}$$

It can be noted that these equations simplifies for a pure Newtonian liquid:

$$\begin{aligned} &G_L' = 0\,; \quad G_L'' \simeq \omega \eta_0' \\ &R_L = X_L \end{aligned} \quad . \tag{16}$$

and a perfect Hookean solid (piezoelectric crystal):

$$\begin{aligned} &G_S'' = 0\,; \quad G_S' \simeq \mu_S \\ &X_S = 0 \end{aligned} \quad , \tag{17}$$

leading to Eq. (11).

If we suppose a single relaxation time, τ_η, and a limiting shear rigidity, G_∞, the complex shear modulus with increasing frequency can be expressed by the Maxwell model [20]:

$$G_L^* = G_L' + jG_L'' = \frac{G_\infty \left(\omega\tau_\eta\right)^2}{1+\left(\omega\tau_\eta\right)^2} + j\frac{\omega\tau_\eta G_\infty}{1+\left(\omega\tau_\eta\right)^2}, \tag{18}$$

and substituting R_L and X_L in Eq. (15), we obtain:

$$\begin{aligned} \eta_L'(f) &= -\frac{\pi}{f_0\rho_L}\left(\frac{Z_Q}{f_0}\right)^2 \frac{\Delta f \Delta\Gamma}{N} = \frac{\tau_\eta G_\infty}{1+\left(2\pi f \tau_\eta\right)^2} \\ \eta_L''(f) &= \frac{\pi}{2 f_0\rho_L}\left(\frac{Z_Q}{f_0}\right)^2 \frac{\Delta\Gamma^2 - \Delta f^2}{N} = -\frac{G_\infty 2\pi f \tau_\eta^2}{1+\left(2\pi f \tau_\eta\right)^2} \end{aligned} \quad . \tag{19}$$

These equations have been used to derive the real and imaginary parts of viscosity from the experimental data. The results obtained for the relaxation spectrum of liquid glycerol are illustrated in Fig. 9. The dashed lines represent the theoretical prediction resulting from a single (Maxwell) relaxation, where the viscous relaxation time, τ_η, has been calculated using the expression [21]:

$$\tau_\eta = \frac{\frac{4}{3}\eta_L + \eta_L^\nu}{\rho_L c_L^2}. \tag{20}$$

η_L and η_L^ν are the shear and volume viscosities, and ρ_L and c_L are the density and sound speed, respectively. This equation shows that the relaxation frequencies decrease with increasing viscosities. For glycerol, the theoretical relaxation time is around 0.5 ns. In Fig. 9, it can be observed that the results obtained clearly follow a relaxational behavior. Nevertheless, the theoretical relaxation time does not exactly fit the experimental data, probably due to the influence of other molecular relaxations not considered in the theoretical approach.

Overall, these results contradict some drawbacks attributed to impulse excitation methods. Actually, it has been shown that not only the spike generation is appropriate for in-liquid applications, but it also offers some unique advantages. In particular, both the real and imaginary parts of the complex resonant frequency can be simultaneously obtained in a wide spectral range (up to 0.25 GHz), which opens the way for spectroscopic analysis. Since it has been seen that the output signals were influenced by unwanted modes, one of the keys to making progress in this area can simply consist in increasing the active surface area of the quartz crystal resonator. In addition, it has been

294 shown that the proposed technique performs better than electrical impedance analysis to
295 characterize highly viscous liquids, such as glycerol, at high frequencies. Moreover,
296 since only the beginning of the signals has to be analyzed, the technique potentially can
297 also be applied in gaseous environments, where reverberation times can be very long.
298 On the other hand, the experiments have been carried out using commercial and
299 general-purpose equipment, and custom-made electronic systems are desirable to
300 compete with oscillator circuits, especially with regard to price, fast response and
301 portability. The advantages and disadvantages of the present excitation method are
302 summarized in Table 2.

303

4 Conclusions

An electronic interface system for thickness-shear piezoelectric resonators (QCM sensors) consisting in a high voltage broadband spike excitation has been described. Contrary to previously assumed limitations, it has been shown that this mode of operation can be successfully applied to simultaneously determine both the resonant frequencies and half bandwidths in a wide spectral range and covering a wide range of liquids. A very good agreement with impedance analysis has been obtained for all the fluids analyzed. Furthermore, promising results at high frequencies open the possibility of developing shear impedance spectrometers based on this approach.

Acknowledgement

This work has been supported by the Spanish Ministry of Science and Innovation (CICYT DPI2010-17716), a CSIC intramural project (ref. 201150E045) and the JAE-CSIC Postdoctoral Program/European Social Fund (JAEDOC2008-065). The authors wish to thank Ricardo T. Higuti for his valuable suggestions.

References

[1] C. Steinem (Ed.), A. Janshoff (Ed.), Piezoelectric Sensors, Springer Series on Chemical Sensors and Biosensors, vol. 5, Springer-Verlag, Heidelberg, 2007.

[2] F. Eichelbaum, R. Borngräber, J. Schröder, R. Lucklum, P. Hauptmann, Interface circuits for quartz-crystal-microbalance sensors, Rev. Sci. Instrum. 70/5 (1999) 2537–2545.

[3] A. Arnau, A Review of interface electronic systems for AT-cut Quartz Crystal Microbalance applications in liquids, Sensors 8 (2008) 370–411.

[4] A. Arnau (Ed.), Piezoelectric Transducers and Applications, second ed., Springer-Verlag, Heidelberg, 2008.

[5] M. Rodahl, F. Höök, A. Krozer, P. Brzezinski, B. Kasemo, Quartz crystal microbalance setup for frequency and Q-factor measurements in gaseous and liquid environments, Rev. Sci. Instrum. 66/7 (1995) 3924–3930.

[6] M. Rodahl, F. Höök, B. Kasemo, QCM operation in liquids: an explanation of measured variations in frequency and Q factor with liquid conductivity, Anal. Chem. 68 (1996) 2219–2227.

[7] M. Rodahl, F. Höök, A. Krozer, B. Kasemo, Piezoelectric crystal microbalance device, US Patent No. 6,006,589 (1999) Dec. 28.

[8] J. Auge, P. Hauptmann, J. Hartmann, S. Rösler, R. Lucklum, New design for QCM sensors in liquids, Sensors and Actuators B 24-25 (1995) 43–48.

[9] J. Schröder, R. Borngräber, F. Eichelbaum, P. Hauptmann, Advanced interface electronics and methods for QCM, Sensors and Actuators A 97-98 (2002) 543–547.

[10] R. Schnitzer, C. Reiter, K.C. Harms, E. Benes, M. Gröschl, A general-purpose online measurement system for resonant BAW sensors, IEEE Sensors J. 6-5 (2006) 1314–1322.

[11] A. Arnau, J.V. García, Y. Jiménez, V. Ferrari, M. Ferrari, Improved electronic interfaces for AT-cut quartz crystal microbalance sensors under variable damping and parallel capacitance conditions, Rev. Sci. Instrum. 79-075110 (2008) 1–12.

[12] M. Ferrari, V. Ferrari, D. Marioli, Interface circuit for multiple-harmonic analysis on quartz resonator sensors to investigate on liquid solution microdroplets, Sensors and Actuators B 146 (2010) 489–494.

[13] P. Resa, C. Sierra, L. Elvira, X-cut quartz crystal impedance meter for liquid characterization, Meas. Sci. Technol. 22 (2011) 025403.

[14] L.W. Schmerr Jr., S.J. Song, Ultrasonic Nondestructive Evaluation Systems, Models and Measurements, Springer Science+Business Media LCC, New York, 2007.

[15] D.R. Lide (ed.), CRC Handbook of Chemistry and Physics, 87th ed., Taylor and Francis Group LLC, Boca Raton, 2006–2007.

[16] H. Nowotny, E. Benes, General one-dimensional treatment of the layered piezoelectric resonator with two electrodes, J. Acoust. Soc. Am. 82/2 (1987), 513–521.

[17] K.K. Kanazawa, J.G. Gordon II, The oscillation frequency of a quartz resonator in contact with a liquid, Anal. Chim. Acta 175 (1985) 99–105.

[18] D. Johannsmann, Viscoelastic analysis of organic thin films on quartz resonators, Macromol. Chem. Phys. 200 (1999) 501–516.

[19] R. Behrends, U. Kaatze, A high frequency shear wave impedance spectrometer for low viscosity liquids, Meas. Sci. Technol. 12 (2001) 519–524.

[20] A.J. Matheson, Molecular Acoustics, Wiley-Interscience, John Wiley & Sons, Bristol, 1971.

[21] A.S. Dukhin, P.J. Goetz, Ultrasound for Characterizing Colloids: Particle Sizing, Zeta Potential, Rheology, Elsevier, Amsterdam, 2002.

List of figure captions

Figure 1. Experimental setup.

Figure 2. A schematic diagram of the experimental cell: (1) AT-cut quartz crystal, (2) electrical connections, (3) panel waterproof connector, (4) container of liquid samples with screw cap, and (5) watertight enclosure with (6) screw-type closure.

Figure 3. Thévenin equivalent circuit for a pulser/receiver connected to a loaded TSM resonator.

Figure 4. Wave pattern of output electrical signals: (a) time and (b) frequency domains.

Figure 5. Linear dependence of the resonant frequency on the square root of the density-viscosity product for several fluids at 25 ºC (fundamental frequency).

Figure 6. Comparison between the resonant frequencies determined by impedance analysis and spike excitation for several fluids at 25 ºC (fundamental frequency; inset: third harmonic).

Figure 7. Relationship between the resonant frequencies and the half bandwidths obtained with the spike excitation method for several fluids at 25 ºC (fundamental frequency).

Figure 8. Frequency dependence of the 'normalized' resonant frequency shifts for several fluids at 25 ºC (relative to pure water). Error bars represent the standard deviation of 5 consecutive signals.

Figure 9. Variation with frequency of the normalized viscosity of glycerol at 25 ºC: experimental (symbols) and theoretical (dashed lines).

Author Biographies:

Pablo Resa López was born in Bilbao in 1976. He holds a M.Sc. degree in Physics from Universidad Autónoma de Madrid (2002) and a Ph.D. degree in Mechanical Engineering from Universidad Politécnica de Madrid (2006). From 2002 to 2006, he worked at the Instituto de Acústica (Consejo Superior de Investigaciones Científicas). In October 2007, he joined the School of Chemistry and Chemical Biology at the University College Dublin. Currently, he is a postdoctoral researcher at the Centro de Acústica Aplicada y Evaluación No Destructiva (UPM-CSIC). His research interests deal with ultrasound-based analytical techniques.

Pedro Castro Blázquez was born in Zaragoza in 1982 (Spain). He holds a B.Sc. in Telecommunications Engineering (2005) and a Master Degree in Transport and Industry Acoustic Engineering (2011) from Universidad Politécnica de Madrid. From 2005 to 2009, he worked as an acoustic engineer in several companies in the sector. In September 2011, he was awarded a fellowship at the Centro de Acústica Aplicada y Evaluación No Destructiva (UPM-CSIC). His main line of research is about ultrasonic characterization techniques based on piezoelectric resonators.

Jaime Rodríguez López was born on 27th February 1984 in Madrid. He received his B.Sc. in Physics from Universidad Complutense de Madrid (UCM, 2007). He also obtained a Master Degree in Material Physics, specialized in nanomaterials (UCM, 2008). Since 2008, he is a Ph.D. fellow at the Centro de Acústica Aplicada y Evaluación No Destructiva (UPM-CSIC). His research interests include the ultrasonic characterization of fluids and magnetorheology.

Luis Elvira Segura was born in Madrid (Spain) on June 30, 1968. He received his B.Sc. and Ph.D. degrees in Physics from the Universidad Complutense de Madrid in 1991 and 1996, respectively. In 2002, he obtained a permanent position at the Instituto de Acústica (CSIC), which becomes Centro de Acústica Aplicada y Evaluación No Destructiva (UPM-CSIC). His research interests are the study of ultrasonic wave propagation in fluids, their applications to the analysis of biological processes and the development of ultrasound-based measuring systems.

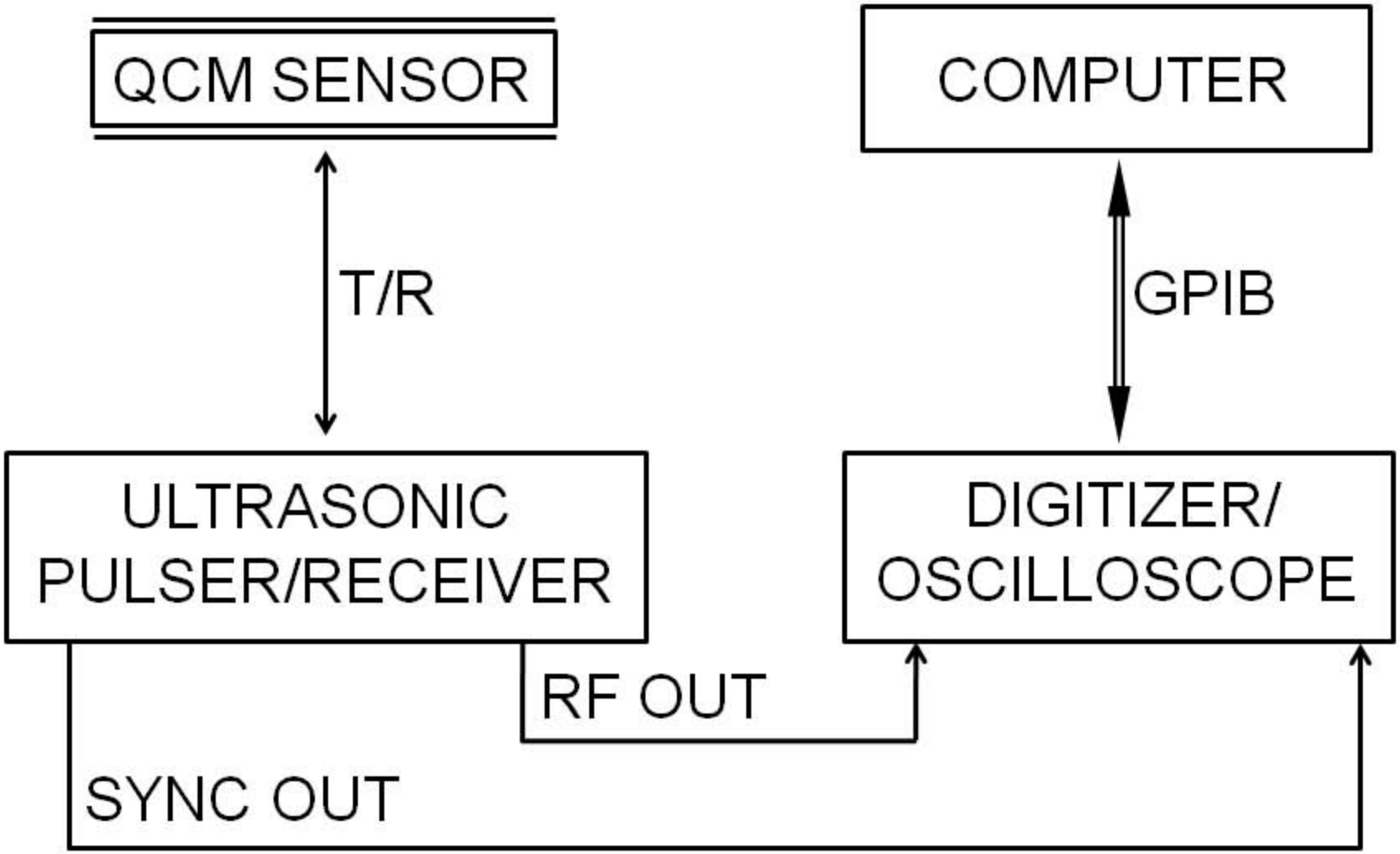
QCM SENSOR
COMPUTER
T/R
GPIB
ULTRASONIC
PULSER/RECEIVER
DIGITIZER/
OSCILLOSCOPE
RF OUT
SYNC OUT

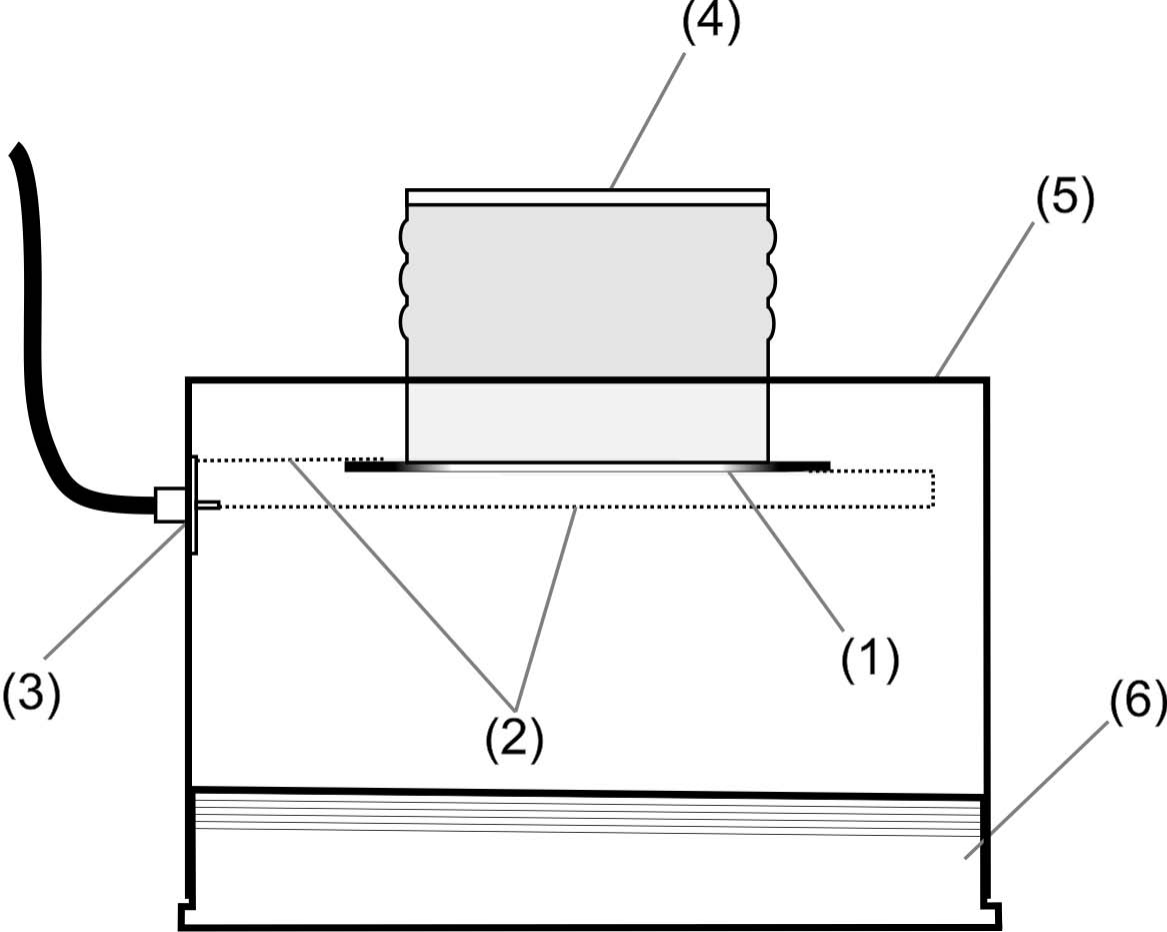
(4)
(5)
(3)
(1)
(2)
(6)

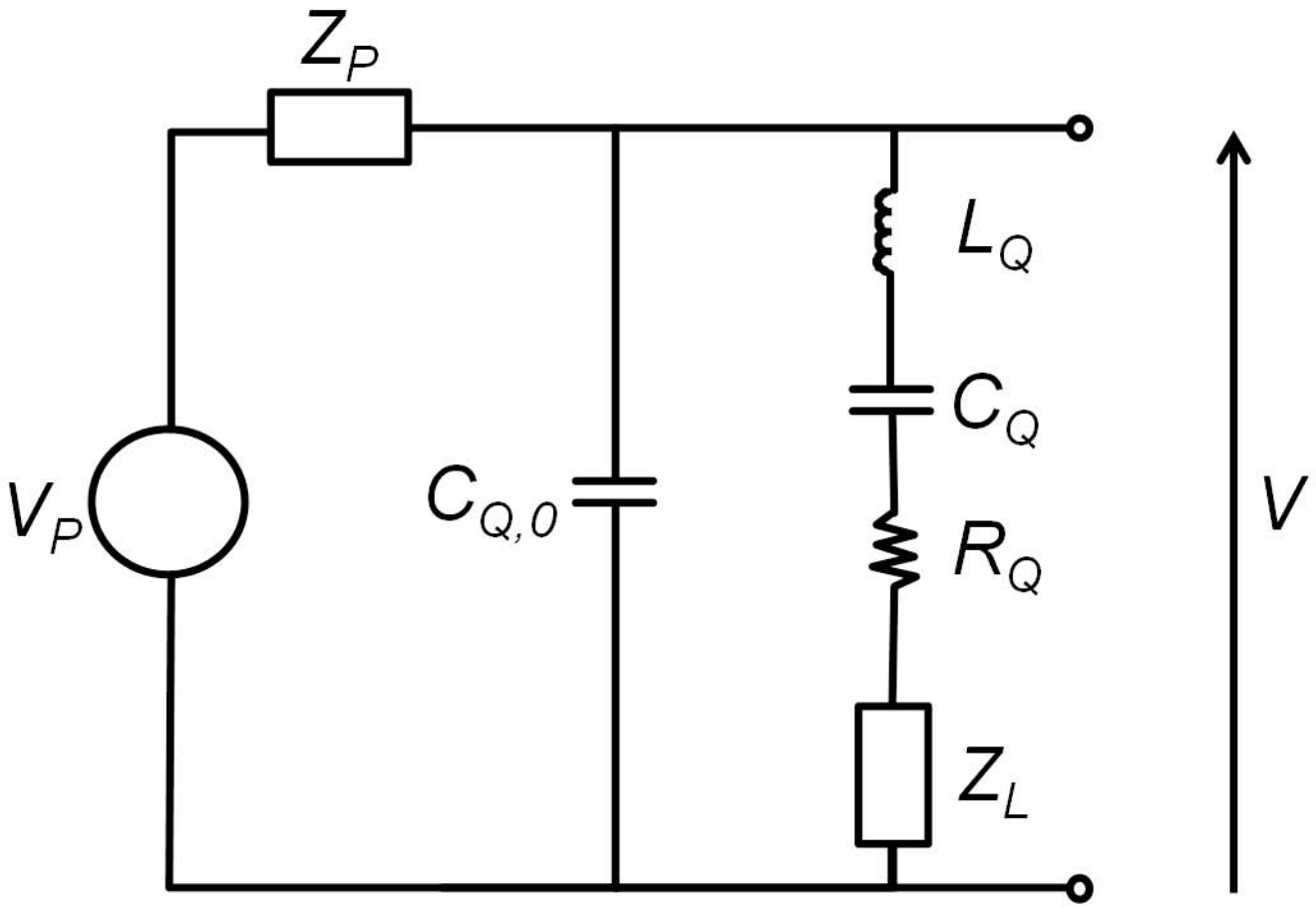
Z_P
L_Q
C_Q
V_P
$C_{Q,0}$
R_Q
V
Z_L

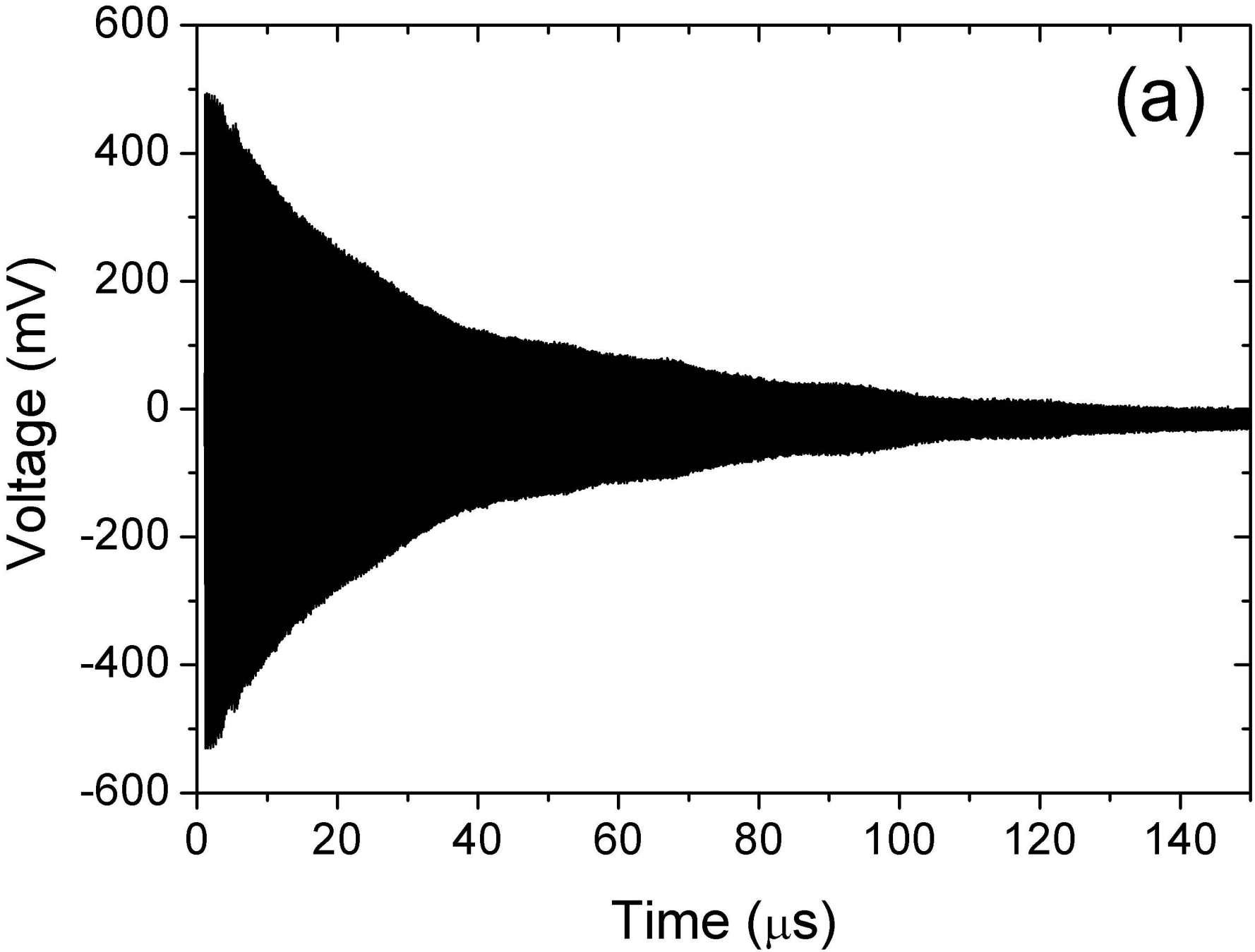
(a)
600
400
200
0
-200
-400
-600
Voltage (mV)
0
20
40
60
80
100
120
140
Time (μs)

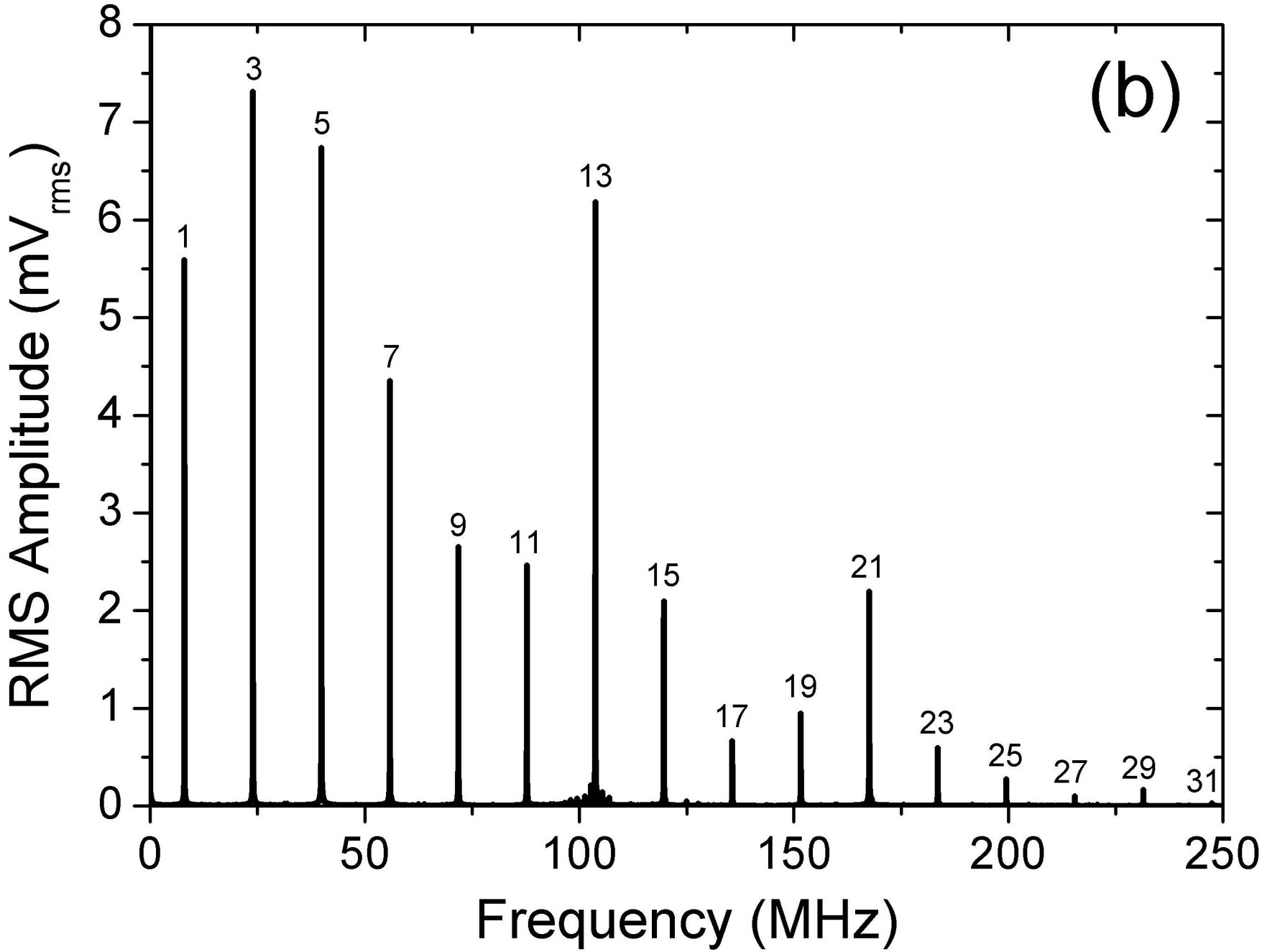
(b)
RMS Amplitude (mV$_{rms}$)
Frequency (MHz)
0
1
2
3
4
5
6
7
8
0
50
100
150
200
250
1
3
5
7
9
11
13
15
17
19
21
23
25
27
29
31

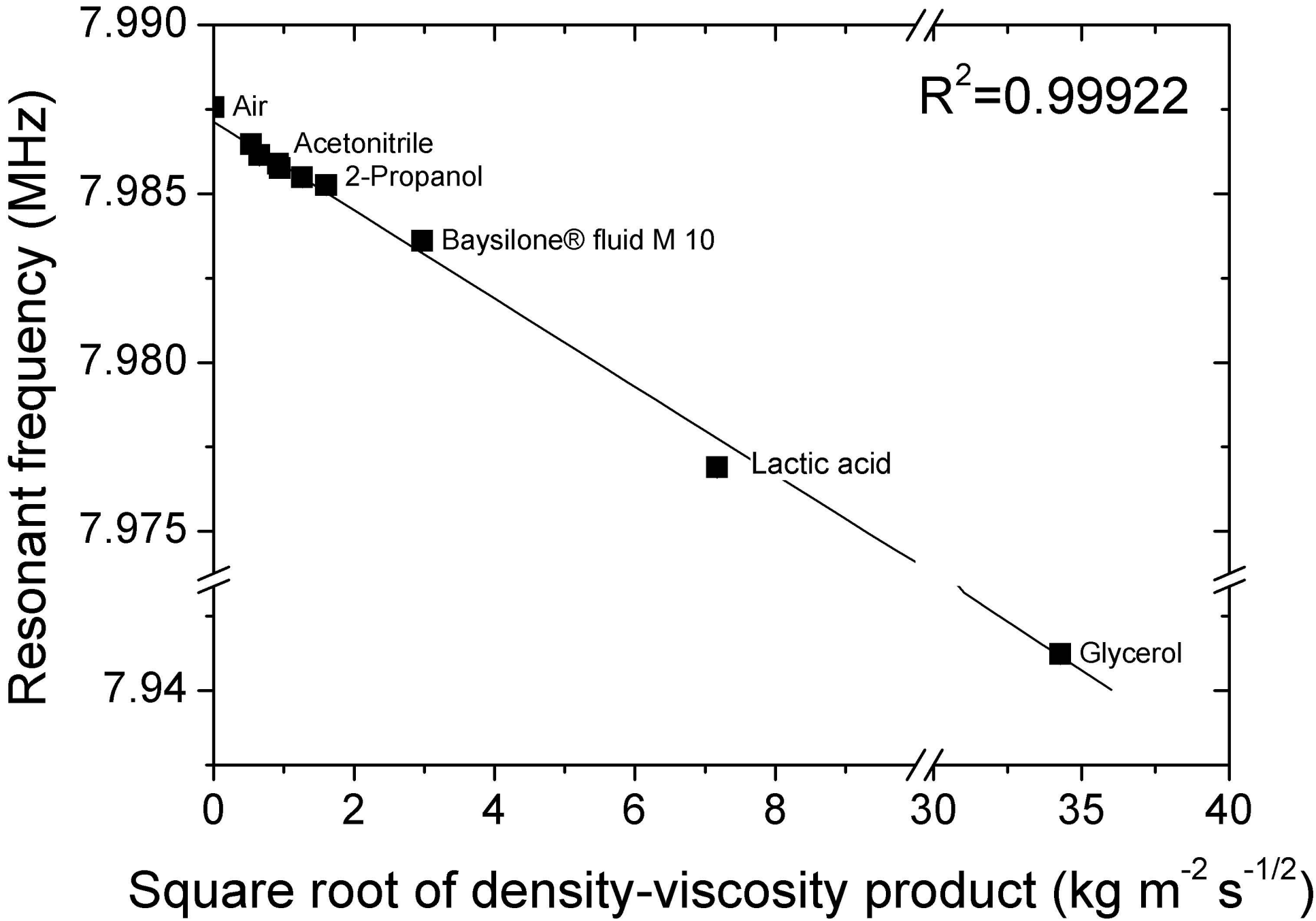
7.990
7.985
7.980
7.975
7.94
Resonant frequency (MHz)
R^2=0.99922
Air
Acetonitrile
2-Propanol
Baysilone® fluid M 10
Lactic acid
Glycerol
0
2
4
6
8
30
35
40
Square root of density-viscosity product (kg m^{-2} s$^{-1/2}$)

IMPEDANCE ANALYSIS

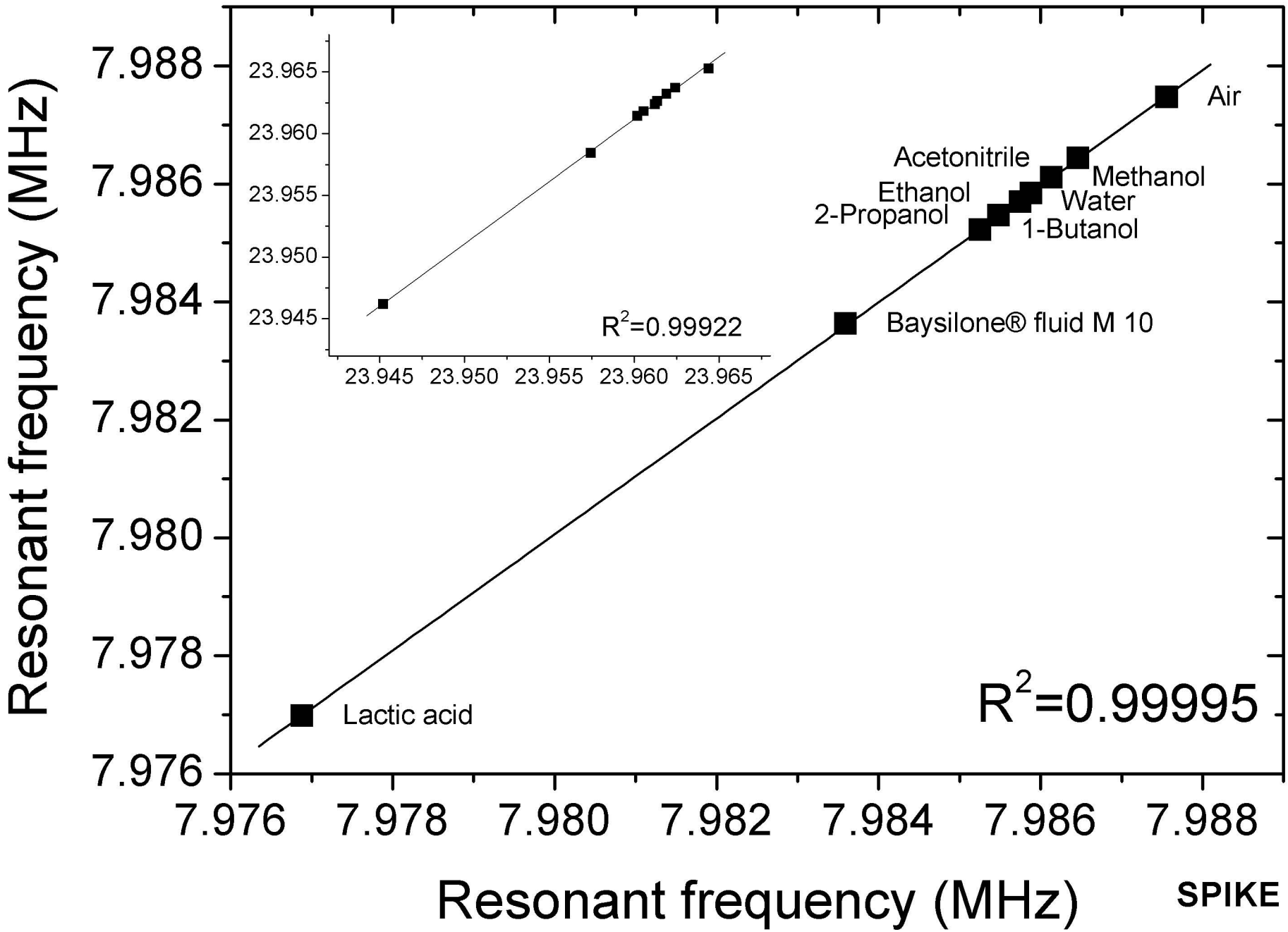

SPIKE METHOD

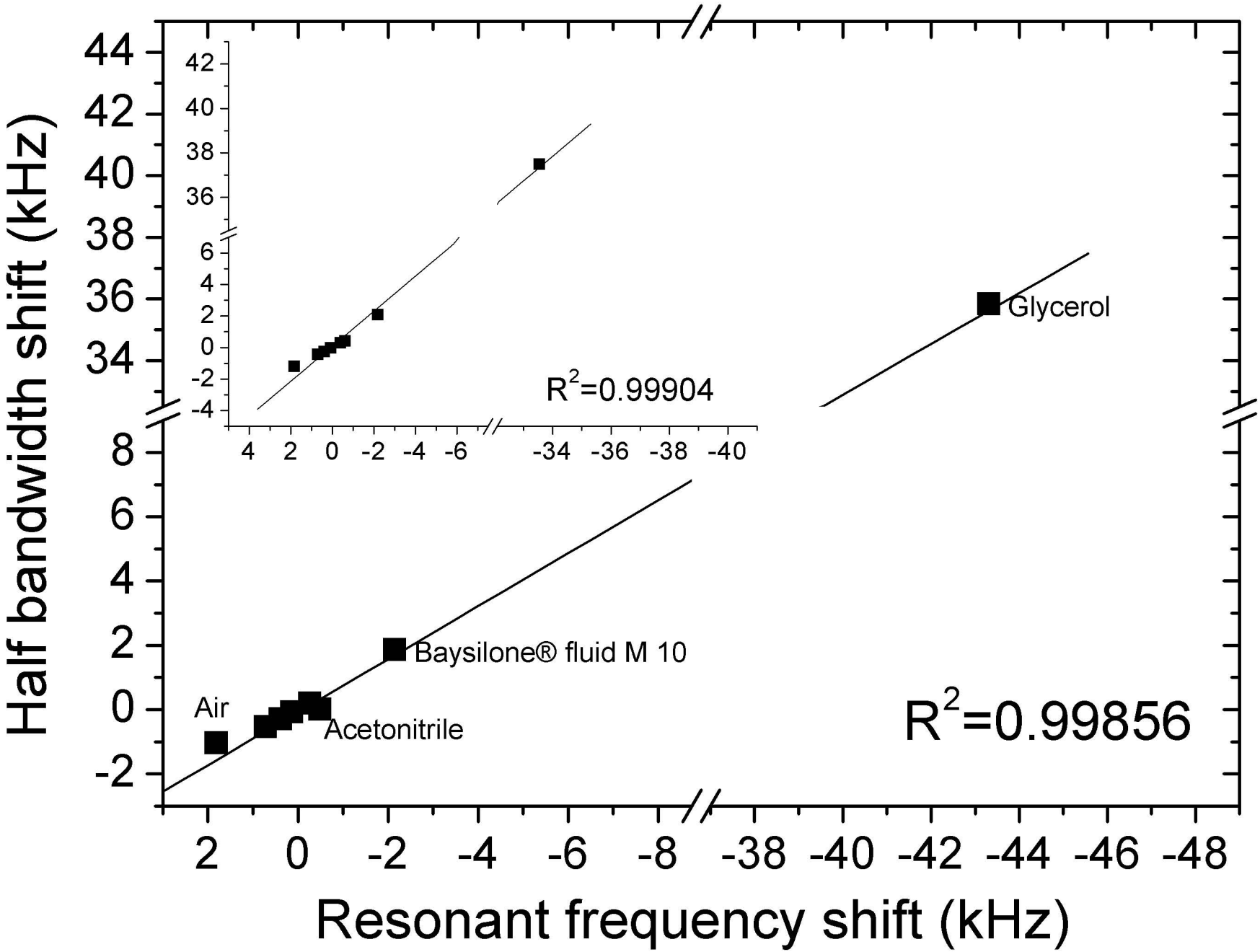
Half bandwidth shift (kHz)
Resonant frequency shift (kHz)
Air
Acetonitrile
Baysilone® fluid M 10
Glycerol
R²=0.99856
R²=0.99904

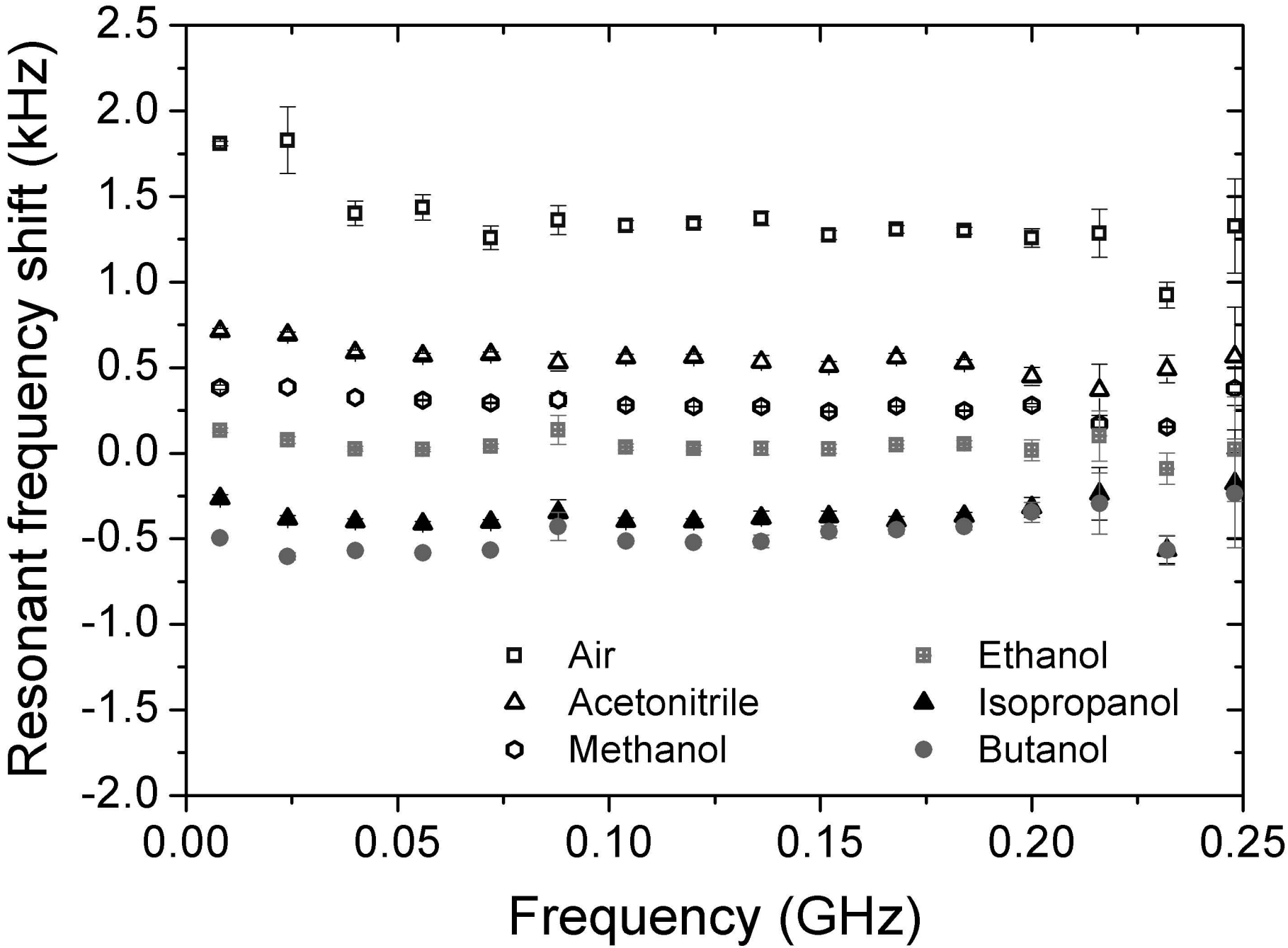
Resonant frequency shift (kHz)
2.5
2.0
1.5
1.0
0.5
0.0
-0.5
-1.0
-1.5
-2.0
0.00
0.05
0.10
0.15
0.20
0.25
Frequency (GHz)
Air
Acetonitrile
Methanol
Ethanol
Isopropanol
Butanol

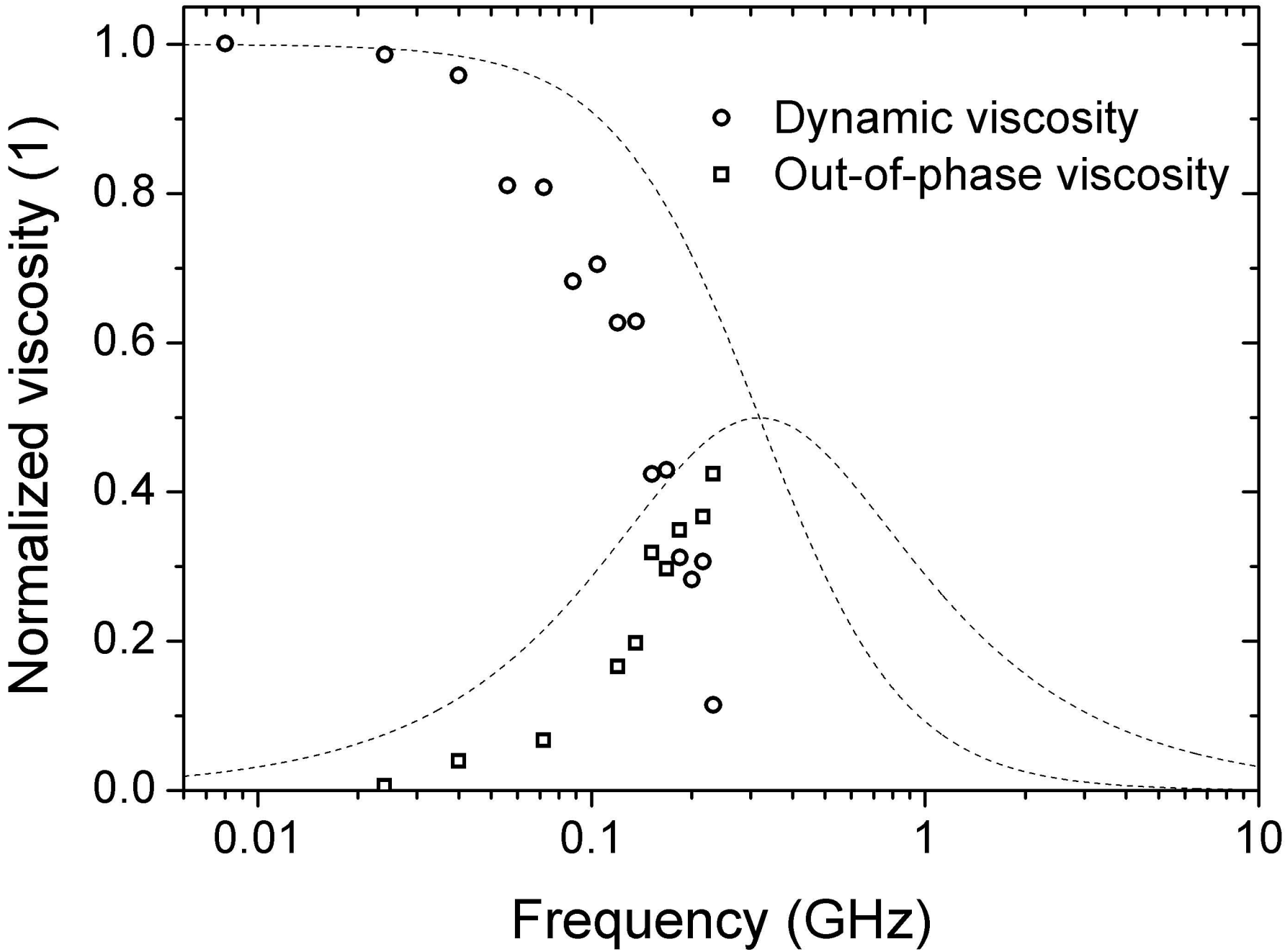
Normalized viscosity (1)
1.0
0.8
0.6
0.4
0.2
0.0
0.01
0.1
1
10
Frequency (GHz)
Dynamic viscosity
Out-of-phase viscosity